iScience

CellPress
OPEN ACCESS

Article

GluN2B S1303 phosphorylation by CaMKII or DAPK1: no indication for involvement in ischemia or LTP

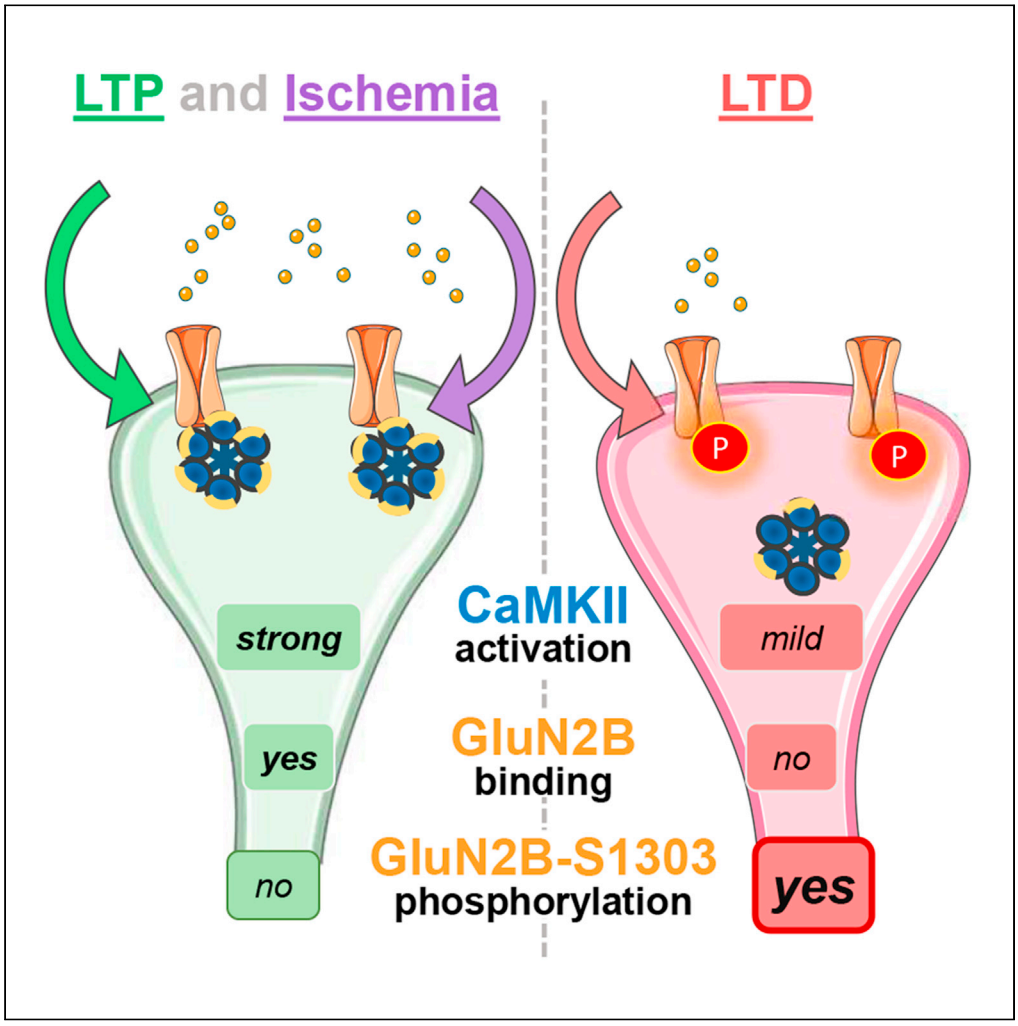

Jonathan E. Tullis, Olivia R. Buonarati, Steven J. Coultrap, ..., Matthew J. Kennedy, Paco S. Herson, K. Ulrich Bayer

paco.herson@osumc.edu (P.S.H.)
ulli.bayer@cuanschutz.edu (K.U.B.)

Highlights

A neuroprotective GluN2B mutation blocked S1303 phosphorylation by CaMKII and DAPK1

GluN2B S1303 is a better substrate for phosphorylation by CaMKII than by DAPK1

Increased phospho-S1303 was detected after cLTD but not cLTP or excitotoxic stimuli

Increased phospho-S1303 was not detected after global cerebral ischemia *in vivo*

Tullis et al., iScience *24*, 103214
October 22, 2021
https://doi.org/10.1016/j.isci.2021.103214

iScience

CellPress
OPEN ACCESS

Article

GluN2B S1303 phosphorylation by CaMKII or DAPK1: no indication for involvement in ischemia or LTP

Jonathan E. Tullis,[1,6] Olivia R. Buonarati,[1,6] Steven J. Coultrap,[1] Ashley M. Bourke,[1,3] Erika L. Tiemeier,[2] Matthew J. Kennedy,[1,5] Paco S. Herson,[1,2,4,5,*] and K. Ulrich Bayer[1,5,7,*]

SUMMARY

Binding of two different CaM kinases, CaMKII and DAPK1, to the NMDA-type glutamate receptor (NMDAR) subunit GluN2B near S1303 has been implicated in excitotoxic/ischemic neuronal cell death. The GluN2B$^{\Delta CaMKII}$ mutation (L1298A, R1300Q) is neuroprotective but abolishes only CaMKII but not DAPK1 binding. However, both kinases can additionally phosphorylate GluN2B S1303. Thus, we here tested S1303 phosphorylation for possible contribution to neuronal cell death. The GluN2B$^{\Delta CaMKII}$ mutation completely abolished phosphorylation by CaMKII and DAPK1, suggesting that the mutation could mediate neuroprotection by disrupting phosphorylation. However, S1303 phosphorylation was not increased by excitotoxic insults in hippocampal slices or by global cerebral ischemia induced by cardiac arrest and cardiopulmonary resuscitation *in vivo*. In hippocampal cultures, S1303 phosphorylation was induced by chemical LTD but not LTP stimuli. These results indicate that the additional effect of the GluN2B$^{\Delta CaMKII}$ mutation on phosphorylation needs to be considered only in LTD but not in LTP or ischemia/excitotoxicity.

INTRODUCTION

The Ca^{2+}/calmodulin-dependent protein kinase II (CaMKII) and the death associated protein kinase 1 (DAPK1) are two related members of the CaM kinase family (reviewed in Bayer and Schulman, 2019). Both kinases can phosphorylate the NMDA-type glutamate receptor (NMDAR) subunit GluN2B at S1303, and both kinases bind to GluN2B near this phosphorylation site (Bayer et al., 2001; Goodell et al., 2017; Strack et al., 2000; Tu et al., 2010). The mutually exclusive competitive nature of CaMKII versus DAPK1 binding to GluN2B is an important determinant of the direction of forms of synaptic plasticity that underly higher brain functions: Normal long-term potentiation (LTP) requires CaMKII binding, which directly enables phosphorylation of the AMPA-type glutamate receptor (AMPAR) subunit GluA1 at S831 (Halt et al., 2012). By contrast, long-term depression (LTD) requires DAPK1 binding, which functions to actively suppress CaMKII binding (Goodell et al., 2017). Despite the mutually exclusive competitive nature of the CaMKII versus DAPK1 binding to GluN2B, binding of both kinases has been implicated in ischemic/excitotoxic neuronal cell death (Buonarati et al., 2020; Tu et al., 2010; Vieira et al., 2015). However, for DAPK1, any involvement in ischemic neuronal cell death has been questioned recently (McQueen et al., 2017) and for CaMKII, functions have been reported not only in neuronal cell death but also in survival (reviewed in Coultrap et al., 2011). Overall, the evidence for a role in neuronal cell death appears in stronger support of CaMKII binding: the GluN2B$^{\Delta CaMKII}$ mutation (L1298A, R1300Q) (Barcomb et al., 2016; Halt et al., 2012) was sufficient to protect neurons from damage by global cerebral ischemia *in vivo*, which appeared to be mediated by abolished GluN2B binding for CaMKII, as DAPK1 binding was unaffected by the mutation (Buonarati et al., 2020). However, this does not formally rule out an additional requirement for DAPK1 and/or an alternative involvement of GluN2B phosphorylation at S1303 by either kinase: as the GluN2B$^{\Delta CaMKII}$ mutation involves two residues located closely to S1303, the mutation could additionally alter phosphorylation efficacy at this site. Indeed, especially the R1300Q mutation would be expected to affect S1303 phosphorylation, as basophilic kinases like CaMKII or DAPK1 have a preference for phosphorylation sites with an upstream basic residue, preferentially arginine (Bayer and Schulman, 2019; Kennelly and Krebs, 1991; Shiloh et al., 2014). Conclusions about the biochemical effect of S1303 phosphorylation on NMDAR function are somewhat conflicting, with the best direct evidence indicating that it reduces NMDAR desensitization

[1]Department of Pharmacology, University of Colorado Anschutz Medical Campus, Aurora, CO 80045, USA

[2]Department of Anesthesiology, University of Colorado Anschutz Medical Campus, Aurora, CO 80045, USA

[3]Program in Neuroscience, University of Colorado Anschutz Medical Campus, Aurora, CO 80045, USA

[4]Present address: Department of Neurosurgery, Ohio State University College of Medicine, Columbus, OH 43210, USA

[5]Present address: Department of Synaptic Plasticity, Max Planck Institute for Brain Research, Frankfurt, Germany

[6]These authors contributed equally

[7]Lead contact

*Correspondence: paco.herson@osumc.edu (P.S.H.), ulli.bayer@cuanschutz.edu (K.U.B.)

https://doi.org/10.1016/j.isci.2021.103214

(Tavalin and Colbran, 2017), whereas more indirect studies had suggested increased NMDAR current (Tu et al., 2010) or increased desensitization (Sessoms-Sikes et al., 2005). Overall, although there are numerous studies indicating the involvement of both CaMKII and DAPK1 in ischemic neuronal cell death (Coultrap et al., 2011; Deng et al., 2017; Pei et al., 2014; Shamloo et al., 2005; Velentza et al., 2003; Vest et al., 2010), it is currently not clear which kinase is more important and if this involves binding to GluN2B and/or GluN2B phosphorylation at S1303.

Here we show that the GluN2B$^{\Delta CaMKII}$ mutation abolishes not only CaMKII binding to GluN2B but also phosphorylation of GluN2B at S1303 by either CaMKII or DAPK1. Nonetheless, the neuroprotective effect of the GluN2B$^{\Delta CaMKII}$ mutation is likely due to preventing CaMKII binding, because an increase in GluN2B S1303 phosphorylation was detected only after LTD stimuli but not after LTP or excitotoxic stimuli *in vitro* or after global cerebral ischemia *in vivo*. Of note, we confirmed that our chemical LTP (cLTP) stimuli indeed caused the expected increase in GluA1 surface expression in hippocampal neurons.

RESULTS

The GluN2B$^{\Delta CaMKII}$ mutation impairs S1303 phosphorylation by CaMKII and DAPK1

The GluN2B$^{\Delta CaMKII}$ mutation combines two point mutations at residues close to S1303, i.e., L1298A and R1300Q (Figure 1A), raising the possibility that it may disrupt not only the binding of CaMKII but also phosphorylation of S1303. Thus, we decided to test the effect of the GluN2B$^{\Delta CaMKII}$ mutation on S1303 phosphorylation. Initial experiments used GST-fusion proteins with the C terminus of the cytoplasmic tail of GluN2B (GluN2Bc; amino acids 1,120–1,482) as substrate for phosphorylation by CaMKII *in vitro*. The GluN2B$^{\Delta CaMKII}$ mutation dramatically reduced phospho-detection by an anti-phospho-S1303 antibody (Figure 1B). However, it was unclear if the reduced phospho-detection was due to impaired phosphorylation by CaMKII or due to reduced ability of antibody to detect the phosphorylation state in the context of a mutated epitope. Thus, we additionally used a phosphorylation assay that detects incorporation of radioactive phosphate into peptide substrates, in this case 18mer peptides corresponding to the GluN2B sequence from amino acid R1295 to K1312 (see Figure 1A). In this assay, this phosphorylation by CaMKII was completely abolished by either GluN2B$^{\Delta CaMKII}$ or S1303A mutation (Figure 1C). Compared with CaMKII, phosphorylation of S1303 by DAPK1 was four orders of magnitude weaker: We detected more than 400 phosphorylation reactions per kinase subunit per minute for CaMKII (Figure 1C), but less than 0.04 reaction per kinase per minute for DAPK1 (Figure 1D). In order to detect reasonable phosphorylation by DAPK1, we used 10x more kinase than for CaMKII (25 nM instead of 2.5 nM) and 30x the reaction time (30 min instead of 1 min). At these reaction times and kinase concentrations, phosphorylation was in the linear range for both CaMKII and DAPK1 (Figure S1). Similar to CaMKII, phosphorylation by DAPK1 was significantly reduced by either GluN2B$^{\Delta CaMKII}$ or S1303A mutation, and the level of phosphorylation for two mutations was indistinguishable (Figure 1D). However, in contrast to CaMKII, phosphorylation by DAPK1 did not appear to be completely abolished, neither for the GluN2B$^{\Delta CaMKII}$ mutation nor for the S1303A mutation (Figure 1D). This is consistent with the much weaker phosphorylation by DAPK1 that may allow an almost comparable detection of phosphorylation of the nearby T1306 that is included in the peptides. In the GST-GluN2B phosphorylation assay that detected S1303 phosphorylation by CaMKII (see Figure 1B), no significant S1303 phosphorylation by DAPK1 was detected at all (Figure S2A).

The apparent difference between CaMKII and DAPK1 could be partially due to differences in the quality of the specific kinase preparations. Thus, we compared the two kinase preparations for phosphorylation of a peptide derived from myosin light chain (MLC), a traditional DAPK1 substrate that is also phosphorylated well by CaMKII. The MLC peptide was phosphorylated about 20-fold better by our CaMKII preparation than by the commercial DAPK1 preparation used here (Figure S2B), indicating that our CaMKII preparation is indeed more active. However, this difference is much smaller than the >10,000-fold difference in phosphorylation rate seen for the GluN2B peptide (see Figures 1C and 1D). More importantly, the DAPK1 preparation phosphorylated the MLC peptide about 200-fold better than the GluN2B peptide (compare Figures 1D and S2B), indicating that GluN2B S1303 is not a very good substrate for DAPK1. By contrast, the GluN2B S1303 phosphorylation by CaMKII was strong: the phosphorylation rate of >400 reactions per minute per kinase (see Figure 1C) is equivalent to the phosphorylation seen for excellent CaMKII substrate peptides (Coultrap et al., 2010; Myers et al., 2017; Woolfrey et al., 2018) and 4-fold higher than seen for the MLC peptide (compare Figure S2B). Most importantly, our results demonstrate that S1303 phosphorylation by either kinase is impaired by the GluN2B$^{\Delta CaMKII}$ mutation, to a similar extent as by S1303A mutation.

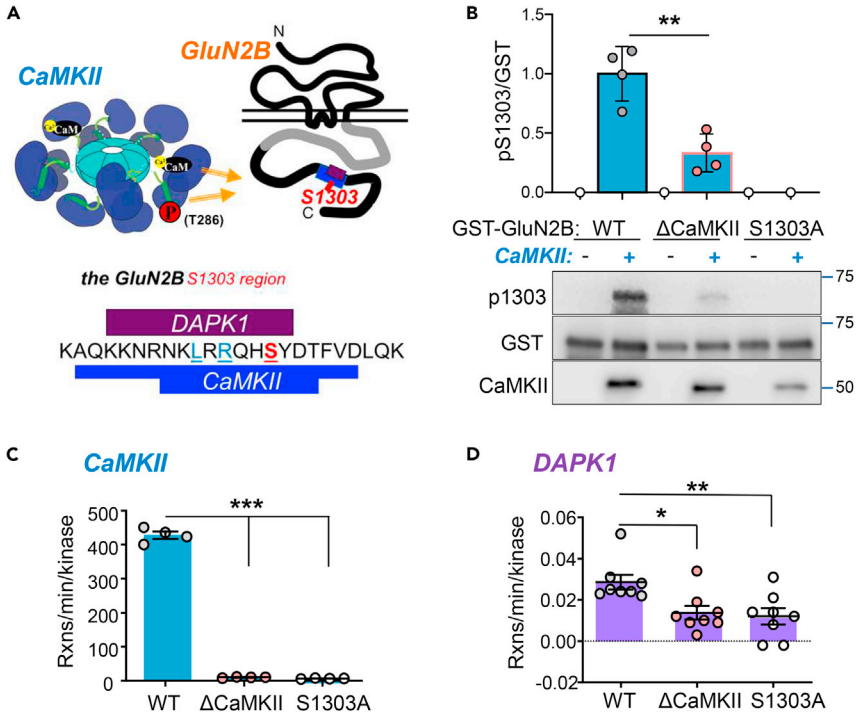

Figure 1. The GluN2BΔCaMKII mutation disrupts S1303 phosphorylation by CaMKII and DAPK1. Error bars indicate SEM in all panels

(A) Schematic of the CaMKII holoenzyme and GluN2B, with S1303 and overlapping binding sites for CaMKII and DAPK1 indicated. CaMKII binding to GluN2B can be induced by Ca^{2+}/CaM or by T286 autophosphorylation. The GluN2B C-tail from amino acids 1,120 to 1,482 was used as substrate in the experiments in B. The shown sequence around S1303 includes the sequences of the peptides used in the experiments in C and D. The residues that were mutated are highlighted: blue for delta CaMKII mutation L1298A, R1300Q; red for the S1303A mutation.

(B) Quantification and representative western blots of *in vitro* kinase reactions between CaMKII and GST-GluN2B proteins. CaMKII phosphorylates GST-GluN2B WT more efficiently than GST-GluN2B$^{\Delta CaMKII}$ (unpaired two-tailed t test: **p = 0.0030; n = 4 reactions per condition).

(C) Incubation of CaMKII (in the presence of Ca^{2+}/CaM) with GluN2B peptides for 1 min induced phosphorylation of GluN2B-WT but not GluN2B-ΔCaMKII or GluN2B-S1303A (one-way ANOVA with Tukey's post hoc: ***p < 0.0001, ns p > 0.05; n = 4 reactions per condition).

(D) Incubation of constitutively active DAPK1 with GluN2B peptides for 30 min induced mild phosphorylation of GluN2B-WT but not GluN2B-ΔCaMKII or GluN2B-S1303A (one-way ANOVA with Tukey's post hoc: *p < 0.05, **p < 0.01, ns p > 0.05; n = 8 reactions per condition).

S1303 phosphorylation is not affected by global cerebral ischemia *in vivo*

Our *in vivo* mouse model for global cerebral ischemia closely resembles the most prevalent human condition: the ischemic cell death that occurs after cardiac arrest, followed by cardiopulmonary resuscitation (CA/CPR). After cardiac arrest for 6 min, CPR is initiated by chest compressions, oxygen supply, and epinephrin (Figure 2A). In this model, the GluN2B$^{\Delta CaMKII}$ mutation provided significant neuroprotection (Buonarati et al., 2020). In order to test if this neuroprotective effect may be due to disruption of S1303 phosphorylation (see Figure 1) rather than disruption of the synaptic CaMKII accumulation that is mediated by GluN2B binding (Buonarati et al., 2020), we decided to test if CA/CPR increases S1303 phosphorylation. Western blot analysis of whole homogenates obtained from hippocampus 2 h after CA/CPR did not indicate any significant increase in GluN2B S1303 phosphorylation in response to the ischemic insult; if any, phosphorylation appeared slightly reduced compared with sham surgery (Figure 2B). In addition, we analyzed crude synaptic versus extrasynaptic fractions for S1303 phosphorylation, in order to detect any potential differences based on subcellular localization; again, no significant differences were detected between CA/CPR versus sham surgery in either of the fractions (Figure 2C). All S1303 phosphorylation signals were normalized to the level of total GluN2B protein (Figures 2B–2E). Of note, total GluN2B protein increased in the synaptic fraction and decreased in the extrasynaptic fraction (Figures 2E and S3A),

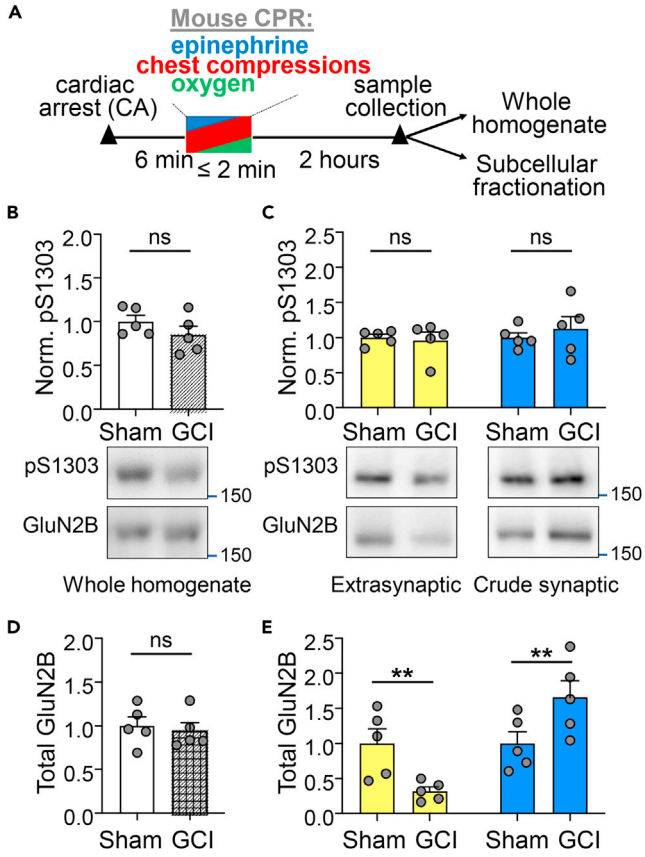

Figure 2. GluN2B S1303 phosphorylation after global cerebral ischemia *in vivo*. Error bars indicate SEM in all panels

(A) Experimental timeline for the CA/CPR model of global cerebral ischemia (GCI). Hippocampi were collected and lysed 2 h after sham or GCI.

(B) Quantification and representative western blots from whole homogenates. No differences in pS1303 were observed between sham and GCI (unpaired two-tailed t test: ns $p = 0.5217$; $n = 5$ mice per condition).

(C) Quantification and representative western blots of extrasynaptic and crude synaptic fractions. As with whole homogenates, no differences in pS1303 were found (two-way ANOVA with Bonferroni's post hoc test: extrasynaptic ns $p = 0.9999$, crude synaptic ns $p = 0.8518$; $n = 5$ mice per condition).

(D) Total GluN2B protein in whole homogenates show no differences between sham and GCI (unpaired two-tailed t test: $p = 0.8912$; $n = 5$ mice per condition).

(E) GluN2B protein is reduced in extrasynaptic fractions and increased in synaptic fractions (two-way ANOVA with Bonferroni's post hoc: extrasynaptic $^{**}p = 0.0011$, synaptic $^{**}p = 0.0014$; $n = 5$ mice per condition).

consistent with our recent report (Buonarati et al., 2020). In summary, the lack of S1303 phosphorylation after CA/CPR indicates that the previously reported neuroprotective effect of the GluN2B$^{\Delta CaMKII}$ is indeed due to disruption of CaMKII binding, as was originally proposed (Buonarati et al., 2020).

S1303 phosphorylation is not affected by excitotoxic insults in hippocampal slices

Similar to results from our *in vivo* model of ischemia, excitotoxic treatment of acute hippocampal slices did not cause a significant change in GluN2B S1303 phosphorylation, neither in the crude synaptic nor the extrasynaptic fraction (Figures 3A and 3B). The excitotoxic insults were induced by 100 μM glutamate for 5 min, and GluN2B S1303 phosphorylation was analyzed both immediately after and 2 h later, with no difference observed in phosphorylation at either time point (Figure 3B). Again, S1303 phosphorylation levels were normalized to total GluN2B protein. The total GluN2B level initially increased in the synaptic fraction but was significantly reduced by 2 h in both fractions (Figures 3B, 3C, and S3B). This decrease in total GluN2B is similar to what we had reported recently after excitotoxic treatments of cultured hippocampal

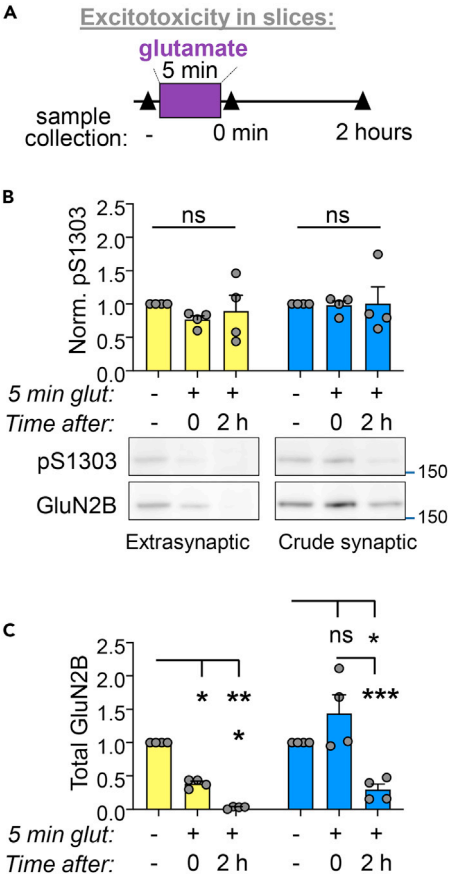

Figure 3. GluN2B S1303 phosphorylation after excitotoxic stimuli in hippocampal slices

Error bars indicate SEM in all panels.

(A) Experimental timeline for the excitotoxic ischemia model in acute hippocampal mouse slices. Slices were collected before, directly after, and 2 h after 100 μm glutamate treatment.

(B) Quantification and representative western blots of extrasynaptic and crude synaptic fractions. No differences in pS1303 were found (two-way ANOVA with Bonferroni's post hoc test: extrasynaptic ns $p = 0.9999$, crude synaptic ns $p = 0.9999$; $n = 4$ slices per condition).

(C) Extrasynaptic GluN2B is dramatically reduced by excitotoxic glutamate (two-way ANOVA with Bonferroni's post hoc test: control versus 5″ glutamate *$p = 0.0262$, control versus 2′ ***$p = 0.0008$, 5″ versus 2′ ns $p = 0.3773$). GluN2B in the crude synaptic fraction decreases 2 h after glutamate (two-way ANOVA with Bonferroni's post hoc test: control versus 5″ ns $p = 0.1612$, control versus 2′ *$p = 0.0103$, 5″ versus 2′ ***$p = 0.0002$; 4 slices per condition).

neurons (Buonarati et al., 2020), although the decrease observed here in hippocampal slices is much more dramatic.

S1303 phosphorylation is increased by chemical LTD but not LTP stimuli in hippocampal cultures

As no increase in S1303 phosphorylation was detected after ischemic insults *in vivo* or after excitotoxic insults in slices, we wanted to make sure that our method was capable of detecting phosphorylation changes in neurons. We had previously shown that S1303 phosphorylation increases after chemical LTD (cLTD) stimuli in hippocampal slices (Goodell et al., 2017). Here, we tested similar cLTD stimuli (30 μM NMDA, 10 μM glycine, and 10 μM CNQX for 3 min) in dissociated hippocampal cultures at 16 days *in vitro* (DIV16) and detected a significant increase in S1303 phosphorylation (Figure 4A), demonstrating feasibility of our detection method. Of importance, the increase in S1303 phosphorylation was LTD specific as no change was seen after a cLTP (100 μM glutamate and 10 μM glycine) stimulus (Figure 4A). Altogether, our data indicate that GluN2B phosphorylation at S1303 is induced by LTD stimuli, but not by LTP stimuli or ischemic/excitotoxic insults.

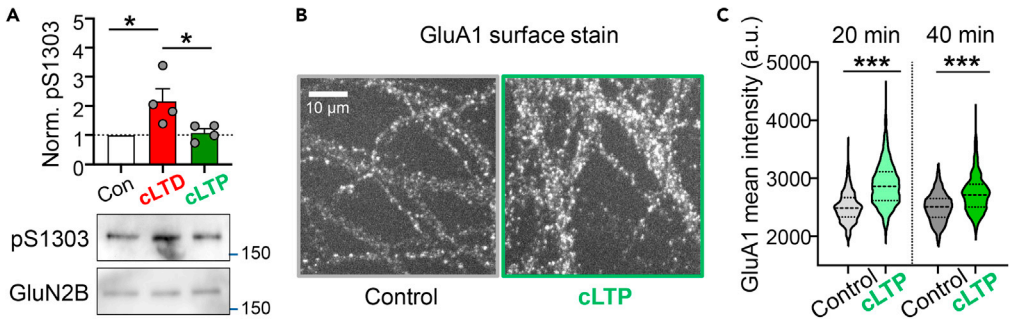

Figure 4. GluN2B S1303 phosphorylation increases after cLTD but not cLTP stimuli

DIV16 hippocampal neurons were treated with cLTP stimuli (100 µM glutamate and 10 µM glycine) or cLTD stimuli (30 µM NMDA, 10 µM glycine, and 10 µM CNQX).

(A) Quantification and representative western blots from whole homogenates prepared immediately after stimulation. Phosphorylation of S1303 increased only after cLTD (one-way ANOVA with Tukey's post hoc test: Con versus cLTD *p = 0.0293, Con versus cLTP ns p = 0.9674, cLTD versus cLTP *p = 0.0430; n = 4 wells per condition)

(B) The effect of the cLTP stimulus was verified by assessing GluA1 surface expression by a live imaging approach.

(C) Quantification of the GluA1 surface expression shows enhanced GluA1 insertion at 20 and 40 min after cLTP compared with after aCSF control; ***p < 0.0001, n = 324 (aCSF), 1,277 (cLTP); unpaired, two-tailed t test.

The chemical LTP stimulation increases surface GluA1 expression

Our cLTD stimulus achieves a mild NMDAR stimulation, as it suppresses AMPAR activation that would cause depolarization and thereby relieve the Mg^{2+} block of NMDARs. By contrast, our cLTP stimulus with 100 µM glutamate and 10 µM glycine achieves a strong NMDAR stimulation, as it causes co-stimulation of AMPARs and thus relieves the Mg^{2+} block. However, the cLTD protocol is well established to cause functional LTD similar to low-frequency electrical stimulation (Carroll et al., 1999; Dudek and Bear, 1992; Lee et al., 1998), whereas the cLTP protocol used here is less well established in its functional effect on synapse strength. In LTP, synapse strength is increased mainly by synaptic incorporation of more AMPARs (Shepherd and Huganir, 2007). Thus, we tested the effect of our cLTP protocol on surface expression of the AMPAR subunit GluA1 using a live-imaging approach (Figures 4B and 4C). Detection of basal GluA1 surface expression was blocked by incubation with an unlabeled GluA1 antibody. Then, only the fresh surface expression of GluA1 after cLTP (or control treatment) was detected with a directly Alexa 647-labeled GluA1 antibody (Figure 4B). GluA1 surface expression was assessed at 20 and 40 min after the cLTP treatment, and a significant increase compared with control was observed at both time points (Figure 4C). Thus, the cLTP stimulus that was used here indeed increases GluA1 surface expression, one of the major cellular mechanisms of LTP expression.

DISCUSSION

We showed here that the neuroprotective GluN2B$^{\Delta CaMKII}$ mutation (L1298A, R1300Q) abolishes not only CaMKII binding (Buonarati et al., 2020) but also CaMKII-mediated phosphorylation of GluN2B at S1303. However, ischemic/excitotoxic insults increase CaMKII binding to synaptic GluN2B (Buonarati et al., 2020), whereas we did not detect any increase in S1303 phosphorylation. This indicates that neuronal cell death is promoted by CaMKII binding to GluN2B but not by its phosphorylation of S1303, and the neuroprotective effect of GluN2B$^{\Delta CaMKII}$ mutation is likely through prevention of this binding. Overall, our findings also provide further indication that CaMKII plays a more important role in ischemic/excitotoxic neuronal cell death than the related CaM kinase, DAPK1. Both CaMKII and DAPK1 bind to GluN2B (Bayer et al., 2001; Strack et al., 2000; Tu et al., 2010), but even though the binding occurs at overlapping sites and is mutually exclusive (Goodell et al., 2017), the neuroprotective GluN2B$^{\Delta CaMKII}$ mutation abolished binding only for CaMKII and not for DAPK1 (Buonarati et al., 2020). Nonetheless, independent from GluN2B binding, several studies support a general role for both CaMKII and DAPK1 in ischemic neuronal cell death (Coultrap et al., 2011; Deng et al., 2017; Pei et al., 2014; Shamloo et al., 2005; Velentza et al., 2003; Vest et al., 2010). However, claims for crucial involvement of DAPK1-mediated phosphorylation of GluN2B at S1303 (Tu et al., 2010) are contradicted by the current study: *In vitro*, S1303 was only minimally phosphorylated by DAPK1 compared with CaMKII. *In vivo*, global cerebral ischemia did not increase S1303 phosphorylation at all, and the same was observed after excitotoxic insults in slices. A similar lack of S1303

phosphorylation after excitotoxic insults has also been reported by others, in a study that argued against any involvement of DAPK1 in ischemic neuronal cell death (McQueen et al., 2017). Thus, overall, the case for involvement in ischemic cell death appears much stronger for CaMKII than for DAPK1. At least GluN2B binding is required only for CaMKII but not DAPK1, and phosphorylation of GluN2B at S1303 does not appear to be involved at all.

Similar as seen after ischemic/excitotoxic stimuli, S1303 phosphorylation was unchanged after LTP stimuli; an increase was seen only after LTD stimuli. Thus, an increase in GluN2B S1303 phosphorylation is inversely correlated with the requirement for CaMKII binding to GluN2B in the process: CaMKII binding is required for normal LTP (Barria and Malinow, 2005; Halt et al., 2012) and for ischemic/excitotoxic neuronal cell death (Buonarati et al., 2020) but not for LTD (Goodell et al., 2017; Halt et al., 2012). Such inverse correlation could have been predicted, as an increase in S1303 phosphorylation decreases CaMKII binding (O'Leary et al., 2011; Strack et al., 2000). Thus, S1303 phosphorylation should not increase during processes that require increased CaMKII binding. By contrast, LTD appears to require active suppression of CaMKII binding to GluN2B (Cook et al., 2021; Goodell et al., 2017), and one of the mechanisms appears to involve the competitive binding of DAPK1 (Goodell et al., 2017). During LTD, this competition for GluN2B binding is tipped in favor of DAPK1 by S1303 phosphorylation, which facilitates DAPK1 binding and reduces CaMKII binding (Goodell et al., 2017).

The GluN2B mutation that was used here disrupts the expression of normal LTP in response to 2 trains of high-frequency stimulation (Halt et al., 2012), whereas a similar mutation with an additional S1303D mutation showed normal LTP in response to theta-burst stimulation (McKay et al., 2018). Our results indicate that the difference between these two studies is due to the different stimulation protocols, rather than involvement of S1303 phosphorylation. This conclusion is also supported by the fact that a similar GluN2B triple mutation that included S1303D did completely abolish LTP in response to a pairing protocol (Barria and Malinow, 2005).

Our results clearly demonstrate that the GluN2B$^{\Delta CaMKII}$ mutation abolishes not only binding of CaMKII (Buonarati et al., 2020) but also phosphorylation of S1303. Thus, both effects need to be taken into account for the interpretations of results with this mutant. However, our results indicate that S1303 phosphorylation increases only after LTD and not after LTP or ischemic/excitotoxic insults. Inversely, CaMKII binding to GluN2B increases after LTP (Bayer et al., 2001; Cook et al., 2021; Halt et al., 2012) and after ischemic/excitotoxic insults (Buonarati et al., 2020) but not after LTD (Cook et al., 2021; Goodell et al., 2017). Thus, the reported effects of the GluN2B$^{\Delta CaMKII}$ mutation on reducing LTP (Halt et al., 2012) and ischemic neuronal cell death (Buonarati et al., 2020) should indeed be due to disrupted CaMKII binding to GluN2B and not to disrupted S1303 phosphorylation. By contrast, the level of LTD is not affected at all by the GluN2B$^{\Delta CaMKII}$ mutation (Goodell et al., 2017; Halt et al., 2012). However, this may well be due to the dual effect of the GluN2B$^{\Delta CaMKII}$ mutation: even though the S1303 phosphorylation that is disrupted by the mutant may be important to inhibit CaMKII binding after LTD stimuli (Goodell et al., 2017), the mutation also directly disrupts CaMKII binding, thereby alleviating the requirement for S1303 phosphorylation to inhibit this CaMKII binding.

If S1303 phosphorylation does not contribute to ischemic/excitotoxic neuronal cell death and if inhibiting CaMKII binding to GluN2B protects from such cell death, then increasing S1303 phosphorylation should also be neuroprotective, as it directly inhibits CaMKII binding (O'Leary et al., 2011; Strack et al., 2000). Thus, it is tempting to speculate that S1303 phosphorylation could be a mechanism for ischemic pre-conditioning, a phenomenon where sub-lethal NMDAR stimuli that are similar to chemical LTD stimuli can provide protection from subsequent toxic NMDAR stimuli. However, this scenario is unlikely, as the increase in S1303 phosphorylation after LTD stimuli is only transient: it is barely detectable after 5 min and fully reversed within 15 min (Goodell et al., 2017).

The increase of S1303 phosphorylation after chemical LTD stimulation has been shown previously in acute hippocampal slices (Goodell et al., 2017) and here in dissociated hippocampal cultures. This LTD stimulation is well established and thought to occur by similar mechanism as the LTD induced by electrical low-frequency stimulation in hippocampal slices or cultures (Carroll et al., 1999; Dudek and Bear, 1992; Lee et al., 1998). By contrast, in acute hippocampal slices, the various cLTP stimulation protocols appear to differ mechanistically from electrical 100-Hz high-frequency stimulation or electrical theta-burst

stimulation. In dissociated hippocampal cultures, the most established cLTP stimulation is induced by removing extracellular Mg^{2+} to alleviate the Mg^{2+} block and adding the NMDAR co-agonist glycine, thereby allowing strong NMDAR stimulation by spontaneous synaptic glutamate release (Liao et al., 2001; Lu et al., 2001). A strength of these low-Mg^{2+} protocols is that they enable LTP induction by synaptic glutamate. However, the reliance on spontaneous glutamate release is also a weakness, as it generates uncertainty about the timing of LTP induction at individual synapses during the prolonged ~5-min induction period. This is not a problem when interrogating the long-lasting effects of LTP, such as the persistent increase in AMPAR surface expression. However, it can be a problem when trying to detect the events that trigger these long-lasting LTP effects but that are themselves transient, such as the likely transient CaMKII activation and T286 autophosphorylation (Bayer and Schulman, 2019). Such transient events may elude biochemical detection in extracts prepared from hippocampal cultures at any time during a low-Mg^{2+} LTP stimulation protocol, as some synapses in the population may have already reversed the event while others may not even have started it. For this reason, many of our previous studies have relied on cLTP stimuli with a 1-min bath application of 100 μM glutamate (in the presence of at least 10 μM glycine to enable NMDAR stimulation by the combination of glutamate and relief of the Mg^{2+} block provided by AMPAR-dependent depolarization). Indeed, this stimulation has LTP-like effects on CaMKII movement to excitatory synapses (Bayer et al., 2001; Cook et al., 2019, 2021). However, the cLTP induction by glutamate bath application is much less established, and our current study is one of the few studies that have demonstrated LTP-like effects also on increasing AMPAR surface expression, which is one of the major functional mediators of LTP. One previous study used immunostaining of fixed cells to show an increase in surface expression for the AMPAR subunit GluA2 (Marsden et al., 2010) (in Figure S6C, which also showed the inverse effect on GluA2 by the chemical LTD protocol with NMDA in the presence of Mg^{2+}). This one precedent is consistent with our observation of increased GluA1 surface expression by live imaging of neurons after cLTP with glutamate. Together, these results provide important confirmation of increased AMPAR surface expression in response to the glutamate-induced cLTP protocol.

One of the most powerful tools to study the physiological and pathological functions of specific biochemical properties of proteins is and remains disrupting these properties by specific mutations. However, in the interpretation of the results, it is always important to consider what additional effects a given mutation may have. Our current study provides an important reminder of this fact, even though it reconfirms the initial conclusions regarding the importance of CaMKII binding to GluN2B rather than phosphorylation of GluN2B S1303 in both LTP (Halt et al., 2012) and ischemic/excitotoxic neuronal cell death (Buonarati et al., 2020). For any additional functional impairment in the GluN2B$^{\Delta CaMKII}$ mutant mice found in future studies, both disrupted CaMKII binding and disrupted S1303 phosphorylation will have to be considered as potential underlying mechanisms.

Limitations of the study

Our results clearly demonstrate that the GluN2B$^{\Delta CaMKII}$ mutation (L1298A, R1300Q) inhibits not only binding of CaMKII but also GluN2B phosphorylation at S1303. However, even though our results additionally indicate that S1303 phosphorylation is not involved in excitatory/ischemic neuronal cell death, such a "negative conclusion" is difficult to demonstrate unequivocally. Specifically, the lack of S1303 phosphorylation at 2 h after CA/CPR *in vivo* or after excitotoxic insults in hippocampal slices *in vitro* does not preclude a temporary increase in S1303 phosphorylation at earlier time points. Occurrence of such a temporary increase appears less likely as no increase in S1303 phosphorylation was detected immediately after the excitotoxic insults either. However, these results do not rule out a temporary increase that occurs with a delay and is then reversed before 2 h. In addition, it is possible that there could be a short-lived temporary increase during the excitotoxic insult that is already reversed by the end of the 5-min insults. Both scenarios appear somewhat unlikely, as no increase in S1303 phosphorylation was observed after cLTP stimulation, which is similar to an excitotoxic insult but shorter in duration. Nonetheless, these possibilities cannot be formally ruled out.

STAR★METHODS

Detailed methods are provided in the online version of this paper and include the following:

- KEY RESOURCES TABLE
- RESOURCES AVAILABILITY
  - Lead contact

SUPPLEMENTAL INFORMATION

Supplemental information can be found online at https://doi.org/10.1016/j.isci.2021.103214.

ACKNOWLEDGMENTS

This work was supported by National Institutes of Health grants F32AG066536 (to O.R.B.), T32GM007635 (supporting J.E.T.), R01NS110383 (to M.J.K. and K.U.B.), R01NS118786 (to P.S.H. and K.U.B), R01NS081248 and R01AG067713 (to K.U.B.).

AUTHOR CONTRIBUTIONS

Conceptualization, J.E.T, O.R.B, S.J.C., M.J.K., P.S.H., and K.U.B.; methodology, J.E.T., A.M.B., and M.J.K.; investigation, J.E.T, O.R.B, S.J.C., A.M.B., and E.L.T.; writing – original draft, K.U.B.; writing – review & editing, J.E.T, O.R.B, S.J.C., A.M.B., E.L.T., M.J.K., P.S.H., and K.U.B.; visualization, J.E.T. O.R.B., P.S.H., and K.U.B.; supervision, M.J.K., P.S.H., and K.U.B.; funding acquisition, O.R.B., M.J.K., P.S.H., and K.U.B.

DECLARATION OF INTERESTS

K.U.B. is co-founder and board member of Neurexis Therapeutics, a company that seeks to develop a CaMKII inhibitor into a therapeutic drug for cerebral ischemia.

Received: June 29, 2021
Revised: July 2, 2021
Accepted: September 29, 2021
Published: October 22, 2021

REFERENCES

Barcomb, K., Hell, J.W., Benke, T.A., and Bayer, K.U. (2016). The CaMKII/GluN2B protein interaction maintains synaptic strength. J. Biol. Chem. *291*, 16082–16089.

Barria, A., and Malinow, R. (2005). NMDA receptor subunit composition controls synaptic plasticity by regulating binding to CaMKII. Neuron *48*, 289–301.

Bayer, K.U., De Koninck, P., Leonard, A.S., Hell, J.W., and Schulman, H. (2001). Interaction with the NMDA receptor locks CaMKII in an active conformation. Nature *411*, 801–805.

Bayer, K.U., and Schulman, H. (2019). CaM kinase: still inspiring at 40. Neuron *103*, 380–394.

Buonarati, O.R., Cook, S.G., Goodell, D.J., Chalmers, N., Rumian, N.L., Tullis, J.E., Restrepo, S., Coultrap, S.J., Quillinan, N., Herson, P.S., et al. (2020). CaMKII versus DAPK1 binding to GluN2B in ischemic neuronal cell death after resuscitation from cardiac arrest. Cell Rep. *30*, 1–8.

Carroll, R.C., Lissin, D.V., von Zastrow, M., Nicoll, R.A., and Malenka, R.C. (1999). Rapid redistribution of glutamate receptors contributes to long-term depression in hippocampal cultures. Nat. Neurosci. *2*, 454–460.

Cook, S.G., Buonarati, O.R., Coultrap, S.J., and Bayer, K.U. (2021). CaMII holoenzyme mechanisms that govern the LTP versus LTD decision. Sci. Adv. *7*, eabe2300.

Cook, S.G., Goodell, D.J., Restrepo, S., Arnold, D.B., and Bayer, K.U. (2019). Simultaneous live imaging of multiple endogenous proteins reveals a mechanism for alzheimer's-related plasticity impairment. Cell Rep. *27*, 658–665 e654, as cover article.

Coultrap, S.J., and Bayer, K.U. (2012). Ca^{2+}/Calmodulin-Dependent protein kinase II (CaMKII). In Neuromethods: Protein Kinase

Technologies, H. Mukai, ed. (Springer), pp. 49–72.

Coultrap, S.J., Buard, I., Kulbe, J.R., Dell'Acqua, M.L., and Bayer, K.U. (2010). CaMKII autonomy is substrate-dependent and further stimulated by Ca2+/calmodulin. J. Biol. Chem. *285*, 17930–17937.

Coultrap, S.J., Vest, R.S., Ashpole, N.M., Hudmon, A., and Bayer, K.U. (2011). CaMKII in cerebral ischemia. Acta Pharmacol. Sin. *32*, 861–872.

Deng, G., Orfila, J.E., Dietz, R.M., Moreno-Garcia, M., Rodgers, K.M., Coultrap, S.J., Quillinan, N., Traystman, R.J., Bayer, K.U., and Herson, P.S. (2017). Autonomous CaMKII activity as a drug target for histological and functional neuroprotection after resuscitation from cardiac arrest. Cell Rep. *18*, 1109–1117.

Dudek, S.M., and Bear, M.F. (1992). Homosynaptic long-term depression in area CA1 of hippocampus and effects of N-methyl-D-aspartate receptor blockade. Proc. Natl. Acad. Sci. U S A *89*, 4363–4367.

Goodell, D.J., Zaegel, V., Coultrap, S.J., Hell, J.W., and Bayer, K.U. (2017). DAPK1 mediates LTD by making CaMKII/GluN2B binding LTP specific. Cell Rep. *19*, 2231–2243.

Halt, A.R., Dallpiazza, R.F., Zhou, Y., Stein, I.S., Qian, H., Juntti, S., Wojcik, S., Brose, N., Silva, A.J., and Hell, J.W. (2012). CaMKII binding to GluN2B is critical during memory consolidation. EMBO J. *31*, 1203–1216.

Hiester, B.G., Bourke, A.M., Sinnen, B.L., Cook, S.G., Gibson, E.S., Smith, K.R., and Kennedy, M.J. (2017). L-type voltage-gated Ca(2+) channels regulate synaptic-activity-triggered recycling endosome fusion in neuronal dendrites. Cell Rep. *21*, 2134–2146.

Kennedy, M.J., Davison, I.G., Robinson, C.G., and Ehlers, M.D. (2010). Syntaxin-4 defines a domain for activity-dependent exocytosis in dendritic spines. Cell *141*, 524–535.

Kennelly, P.J., and Krebs, E.G. (1991). Consensus sequences as substrate specificity determinants for protein kinases and protein phosphatases. J. Biol. Chem. *266*, 15555–15558.

Lee, H.K., Kameyama, K., Huganir, R.L., and Bear, M.F. (1998). NMDA induces long-term synaptic depression and dephosphorylation of the GluR1 subunit of AMPA receptors in hippocampus. Neuron *21*, 1151–1162.

Liao, D., Scannevin, R.H., and Huganir, R. (2001). Activation of silent synapses by rapid activity-dependent synaptic recruitment of AMPA receptors. J. Neurosci. *21*, 6008–6017.

Lu, W., Man, H., Ju, W., Trimble, W.S., MacDonald, J.F., and Wang, Y.T. (2001). Activation of synaptic NMDA receptors induces membrane insertion of new AMPA receptors and LTP in cultured hippocampal neurons. Neuron *29*, 243–254.

Marsden, K.C., Shemesh, A., Bayer, K.U., and Carroll, R.C. (2010). Selective translocation of Ca2+/calmodulin protein kinase IIalpha (CaMKIIalpha) to inhibitory synapses. Proc. Natl. Acad. Sci. U S A *107*, 20559–20564.

McKay, S., Ryan, T.J., McQueen, J., Indersmitten, T., Marwick, K.F.M., Hasel, P., Kopanitsa, M.V., Baxter, P.S., Martel, M.A., Kind, P.C., et al. (2018). The developmental shift of NMDA receptor composition proceeds independently of GluN2 subunit-specific GluN2 C-terminal sequences. Cell Rep. *25*, 841–851 e844.

McQueen, J., Ryan, T.J., McKay, S., Marwick, K., Baxter, P., Carpanini, S.M., Wishart, T.M., Gillingwater, T.H., Manson, J.C., Wyllie, D.J.A., et al. (2017). Pro-death NMDA receptor signaling is promoted by the GluN2B C-terminus independently of Dapk1. Elife *6*, e17161.

Myers, J.B., Zaegel, V., Coultrap, S.J., Miller, A.P., Bayer, K.U., and Reichow, S.L. (2017). The CaMKII holoenzyme structure in activation-competent conformations. Nat. Commun. *8*, 15742.

O'Leary, H., Liu, W.H., Rorabaugh, J.M., Coultrap, S.J., and Bayer, K.U. (2011). Nucleotides and phosphorylation bi-directionally modulate Ca2+/calmodulin-dependent protein kinase II (CaMKII) binding to the N-methyl-D-aspartate (NMDA) receptor subunit GluN2B. J. Biol. Chem. *286*, 31272–31281.

Orfila, J.E., Shimizu, K., Garske, A.K., Deng, G., Maylie, J., Traystman, R.J., Quillinan, N., Adelman, J.P., and Herson, P.S. (2014). Increasing small conductance Ca2+-activated potassium channel activity reverses ischemia-induced impairment of long-term potentiation. Eur. J. Neurosci. *40*, 3179–3188.

Pei, L., Shang, Y., Jin, H., Wang, S., Wei, N., Yan, H., Wu, Y., Yao, C., Wang, X., Zhu, L.Q., et al. (2014). DAPK1-p53 interaction converges necrotic and apoptotic pathways of ischemic neuronal death. J. Neurosci. *34*, 6546–6556.

Sessoms-Sikes, S., Honse, Y., Lovinger, D.M., and Colbran, R.J. (2005). CaMKIIalpha enhances the desensitization of NR2B-containing NMDA receptors by an autophosphorylation-dependent mechanism. Mol. Cell. Neurosci. *29*, 139–147.

Shamloo, M., Soriano, L., Wieloch, T., Nikolich, K., Urfer, R., and Oksenberg, D. (2005). Death-associated protein kinase is activated by dephosphorylation in response to cerebral ischemia. J. Biol. Chem. *280*, 42290–42299.

Shepherd, J.D., and Huganir, R.L. (2007). The cell biology of synaptic plasticity: AMPA receptor trafficking. Annu. Rev. Cell Dev. Biol. *23*, 613–643.

Shiloh, R., Bialik, S., and Kimchi, A. (2014). The DAPK family: a structure-function analysis. Apoptosis *19*, 286–297.

Shimizu, K., Quillinan, N., Orfila, J.E., and Herson, P.S. (2016). Sirtuin-2 mediates male specific neuronal injury following experimental cardiac arrest through activation of TRPM2 ion channels. Exp. Neurol. *275* (Pt 1), 78–83.

Singla, S.I., Hudmon, A., Goldberg, J.M., Smith, J.L., and Schulman, H. (2001). Molecular characterization of calmodulin trapping by calcium/calmodulin-dependent protein kinase II. J. Biol. Chem. *276*, 29353–29360.

Strack, S., McNeill, R.B., and Colbran, R.J. (2000). Mechanism and regulation of calcium/calmodulin-dependent protein kinase II targeting to the NR2B subunit of the N-methyl-D-aspartate receptor. J. Biol. Chem. *275*, 23798–23806.

Tavalin, S.J., and Colbran, R.J. (2017). CaMKII-mediated phosphorylation of GluN2B regulates recombinant NMDA receptor currents in a chloride-dependent manner. Mol. Cell. Neurosci. *79*, 45–52.

Tu, W., Xu, X., Peng, L., Zhong, X., Zhang, W., Soundarapandian, M.M., Balel, C., Wang, M., Jia, N., Lew, F., et al. (2010). DAPK1 interaction with NMDA receptor NR2B subunits mediates brain damage in stroke. Cell *140*, 222–234.

Velentza, A.V., Wainwright, M.S., Zasadzki, M., Mirzoeva, S., Schumacher, A.M., Haiech, J., Focia, P.J., Egli, M., and Watterson, D.M. (2003). An aminopyridazine-based inhibitor of a pro-apoptotic protein kinase attenuates hypoxia-ischemia induced acute brain injury. Bioorg. Med. Chem. Lett. *13*, 3465–3470.

Vest, R.S., O'Leary, H., Coultrap, S.J., Kindy, M.S., and Bayer, K.U. (2010). Effective post-insult neuroprotection by a novel Ca(2+)/calmodulin-dependent protein kinase II (CaMKII) inhibitor. J. Biol. Chem. *285*, 20675–20682.

Vieira, M.M., Schmidt, J., Ferreira, J.S., She, K., Oku, S., Mele, M., Santos, A.E., Duarte, C.B., Craig, A.M., and Carvalho, A.L. (2015). Multiple domains in the C-terminus of NMDA receptor GluN2B subunit contribute to neuronal death following in vitro ischemia. Neurobiol. Dis. *89*, 223–234.

Woolfrey, K.M., O'Leary, H., Goodell, D.J., Robertson, H.R., Horne, E.A., Coultrap, S.J., Dell'Acqua, M.L., and Bayer, K.U. (2018). CaMKII regulates the depalmitoylation and synaptic removal of the scaffold protein AKAP79/150 to mediate structural long-term depression. J. Biol. Chem. *293*, 1551–1567.

STAR★METHODS

KEY RESOURCES TABLE

REAGENT or RESOURCE	SOURCE	IDENTIFIER
Antibodies		
CaMKIIα	Made in House	CBα2; RRID: AB_2533032
CaMKIIα pT286	Phospho-Solutions	p1005-286; RRID: AB_2492051
DAPK1	Sigma	D1319; RRID: AB_1078622
GluN2B	Cell Signaling	D8E10; RRID: AB_2798506
GluN2B pS1303	Millipore	07-398; RRID: AB_310582
GluA1	Laboratory of Matthew Kennedy	
GST	Millipore	AB3282; RRID: AB_91439
Beta Actin	Cell Signaling	13E5; RRID: AB_2223172
PSD95	Neuromab	73-028; RRID: AB_10698024
Goat anti-Rabbit	GE Healthcare	NA934V; RRID: AB_772206
Goat anti-Mouse	GE Healthcare	NA931V; RRID: AB_772210
Chemicals, peptides, and recombinant proteins		
Papain	Worthington	LS 03126
Lipofectamine 2000	Invitrogen	11668027
B-27 supplement	Gibco	17504044
Glutamate	Sigma	6106-04-3
Glycine	Sigma	56-40-6
CNQX	Sigma	115066-14-3
cOmplete protease inhibitor cocktail (EDTA-free)	Roche	1187380001
Microcystin-LR	Calbiochem	475815
Calmodulin	Made in house	CaM
Ca^{2+}/CaM-dependent kinase II α	Made in house	CaMKII
GST-GluN2B C-tail	Made in house	GST-GluN2Bc
GST-GluN2B S1303A	Made in house	GST-GluN2Bc 1303A
GST-GluN2B$^{\Delta CaMKII}$	Made in house	GST-GluN2Bc$^{\Delta CaMKII}$
GluN2B peptide- RNKLRRQHSYDTFVDLQK	Chi Scientific	GluN2B-WT
GluN2B peptide- RNKLRRQHAYDTFVDLQK	Chi Scientific	GluN2B-S1303A
GluN2B peptide- RNKARQQHSYDTFVDLQK	Chi Scientific	GluN2B-ΔCaMKII
MLC peptide-KKRPQRRYSNVF	Tocris	1458 (also termed "DAPK Substrate peptide")
Critical commercial assays		
Pierce BCA protein assay	Thermo-Fisher	23225
SuperSignal West Femto	Thermo Fisher	34095
Deposited data		
Raw and analyzed data	This paper	Mendeley Data: https://doi.org/10.17632/2pyx7n8wvp.1
Experimental models: Cell lines		
Primary hippocampal cultures	Laboratory of K. Ulrich Bayer	N/A
Experimental models: Organisms/strains		
Mouse: wild type: C57BL/6	Charles River Labs	
Rat: Sprague-Dawley	Charles River Labs	N/A

(*Continued on next page*)

Continued

REAGENT or RESOURCE	SOURCE	IDENTIFIER
Software and algorithms		
Slidebook 6.0	Intelligent Imaging Innovations (3i)	RRID:SCR_014300
Prism 7.0	Graphpad	RRID: SCR_002798
AlphaEase FC 4.0	Alpha Innotech	N/A
ImageJ	NIH	RRID:SCR_003070

RESOURCES AVAILABILITY

Lead contact

The Lead contact is K. Ulrich Bayer (ulli.bayer@cuanschutz.edu).

Materials availability

Further information and requests for resources and reagents should be directed to and will be fulfilled by the lead contact. This study did not generate new unique reagents.

Code and data availability

- Data have been deposited at Mendeley and are publicly available as of the date of publication. Accession numbers are listed in the key resources table.
- Images were analyzed without the need for original code. Basic thresholding using imageJ were implemented to measure intensity of GluA1 puncta.

EXPERIMENTAL MODEL AND SUBJECT DETAILS

All animal treatment was approved by the University of Colorado Institutional Animal Care and Use Committee (IACUC), in accordance with NIH guidelines (see also Buonarati et al., 2020). Animals are housed at the Animal Resource Center at the University of Colorado Anschutz Medical Campus (Aurora, CO) and are regularly monitored with respect to general health, cage changes, and overcrowding. Pregnant Sprague-Dawley rats were supplied by Charles River Labs. Male C57BL/6 adult mice, 8 to 12 weeks old, were also supplied by Charles River Labs.

METHOD DETAILS

Material and DNA constructs

Material was obtained from Sigma, unless noted otherwise. The DAPK1 was N-terminal GST-tagged, recombinant, human DAPK1 (amino acids 1-296) and was purchased from EMD Millipore (cat# 14-692). The 2B-C peptides were custom synthesized by Chi Scientific (WT: RNKLRRQHSYDTFVDLQK; S1303A: RNKLRRQHAYDTFVDLQK; and ΔCaMKII: RNKARQQHSYDTFVDLQK). The DAPK1 substrate peptide was purchase from Tocris (KKRPQRRYSNVF).

Protein purification

CaMKIIα was purified from a baculovirus/Sf9 cell expression system; CaM and GST-GluN2Bc WT and mutant constructs were purified from BL21 bacteria

(see also Bayer et al., 2001; Cook et al., 2021; Coultrap and Bayer, 2012; Singla et al., 2001).

Western analysis

Protein concentration was determined using the Pierce BCA protein assay (Thermo-Fisher). Before undergoing SDS-PAGE, samples were boiled in Laemmli sample buffer for 5 min at 95°C. Proteins were separated in a resolving phase polymerized from 7.5% acrylamide, then transferred to a polyvinylidene difluoride membrane at 24 V for 1-2 h at 4°C. Membranes were blocked in 5% milk or BSA and incubated with anti-CaMKIIα (1:4000, CBα2, available at Invitrogen but made in house), pT286-CaMKII (1:2500, Phospho-Solutions), anti-GluN2B (1:1000, Cell Signaling), pS1303-GluN2B (1:250, Millipore), DAPK1 (1:800, Sigma-Aldrich), or PSD95 (1:1000, Neuromab) followed by either Amersham ECL goat anti-mouse

HRP-linked secondary 1:10000 (GE Healthcare) or goat anti-rabbit horseradish peroxidase conjugate 1:10000 (Bio-Rad). Blots were developed using chemiluminescence (Super Signal West Femto, Thermo-Fisher), imaged using the Chemi-Imager 4400 system (Alpha-Innotech), and analyzed by densitometry (ImageJ). GluN2B S1303 phospho-signal was corrected to total GluN2B protein. Quantification of relative GluN2B protein levels in the fractions was based on equal loading, with minor variations in sample loading corrected using β-actin (1:2000, Cell Signaling). Relative band intensity was normalized as a percent of control conditions on the same blot, which was set at a value of one to allow for comparison between multiple experiments.

Phosphorylation of GST-GluN2Bc *in vitro*

CaMKII-mediated phosphorylation of GluN2B S1303 was measured by *in vitro* kinase reaction with purified GST-GluN2Bc (WT, ΔCaMKII, S1303A). Reactions contained 40 nM CaMKII (or 200 nM DAPK1, or water for negative controls), 1 μM GST-GluN2Bc, 50 mM PIPES pH 7.1, 2 mM $CaCl_2$, 10 mM $MgCl_2$, 1 μM calmodulin, 2 mM ATP, and 1 μM of okadaic acid. Reactions were done at 30°C for 20 seconds, and stopped by adding SDS-loading buffer and incubation in a boiling water bath for 5 min. For DAPK1 reaction the time was extended to 10 min. GST, phospho-S1303, and CaMKII were detected in the samples by Western analysis.

Radioactive kinase assays

Standard CaMKII reactions were done for 1 min at 30°C and started by adding CaMKIIα (2.5 nM subunits, unless stated otherwise) to a mix of 50 mM PIPES pH 7.1, 0.1% BSA, 1 μM CaM, 1 mM $CaCl_2$, 10 mM $MgCl_2$, 100 μM [γ-^{32}P]ATP (~1 Ci/mmole), 6 μM GluN2B substrate peptide (2B-C WT, ΔCaMKII, or S1303A) (see also Coultrap and Bayer, 2012; Coultrap et al., 2010). Concentrated constitutively active DAPK1 (amino acids 1-296) was diluted to a 5X working solution with DAPK1 dilution buffer (20 mM PIPES pH 7.1, 1 mM EDTA, 5% glycerol, 0.1% β-mercaptoethanol, 1 mg/ml BSA, 0.01% Tween-20). DAPK1 reactions (30 min at 30°C) were started by adding DAPK1 (25 nM) to a mix of 50 mM PIPES pH 7.1, 0.1% BSA, 0.5 mM EDTA, 10 mM $MgCl_2$, 100 μM [γ-^{32}P]ATP (~1 Ci/mmole), 6 μM GluN2B substrate peptide (2B-C WT, ΔCaMKII, or S1303A). For the MLC-derived DAPK substrate peptide, 100 μM was used. For all kinase activity assays, reactions were stopped by spotting onto P81 cation exchange chromatography paper (Whatman) squares. After extensive washes in water, phosphorylation of the substrate peptide bound to the P81 paper was measured by submersing in Bio-safe N/A scintillation fluid and counting in a liquid scintillation counter.

Protein extracts and fractionation

Whole homogenates of hippocampi or cultured hippocampal neurons were solubilized in 1% SDS buffer also containing (in mM): 10 Tris, 10 EDTA, 10 EGTA, 150 NaCl, plus protease and phosphatase inhibitors, and cleared by centrifugation for 20 min at room temperature.

Fractions from acute hippocampal slices or hippocampi were homogenized as follows: To make the extra-synaptic fraction, cells were homogenized in ice-cold 1% TX100 buffer also containing (in mM): 10 Tris, 10 EDTA, 10 EGTA, 150 NaCl, plus protease and phosphatase inhibitors and cleared by ultracentrifugation (100,000 x g) for 30 min at 4°C. To make the crude synaptic fraction, the remaining insoluble pellet (including synaptosomes and lipid rafts) was solubilized in 1% SDS buffer also containing (in mM): 10 Tris, 10 EDTA, 10 EGTA, 150 NaCl, plus protease and phosphatase inhibitors, then heated at 65°C for 15 min, quenched with 1.5% TX100, and cleared by centrifugation (20,000 x g) for 20 min.

CA/CPR

For cardiac arrest and cardiopulmonary resuscitation (CA/CPR), asystolic cardiac arrest was induced by KCl injection via jugular catheter, and 6 min later, CPR was initiated by injecting 0.5-1 mL epinephrine (16 mg/mL in saline solution), chest compressions at 300/min, and ventilation with 100% O_2 (see also Buonarati et al., 2020; Deng et al., 2017; Orfila et al., 2014; Shimizu et al., 2016). If return of spontaneous circulation was not achieved within 2 min of CPR, the animal was excluded from the study. Tissue from was collected 2 h after CA/CPR for Western analysis of GluN2B phosphorylation in the hippocampus.

Excitotoxic insult in acute hippocampal slices

Hippocampal slices were prepared using WT mice (8-12 weeks old). Isoflurane anesthetized mice were rapidly decapitated, and the brain was dissected in ice-cold high sucrose solution containing (in mM): 220 sucrose, 12 $MgSO_4$, 10 glucose, 0.2 $CaCl_2$, 0.5 KCl, 0.65 NaH_2PO_4, 13 $NaHCO_3$, and 1.8 ascorbate.

Transverse hippocampal slices (400 μm) were made using a tissue chopper (McIlwain) and transferred into 32°C artificial cerebral spinal fluid (ACSF) containing (in mM): 124 NaCl, 2 KCl, 1.3 NaH_2 PO4, 26 $NaHCO_3$, 10 glucose, 2 $CaCl_2$, 1 $MgSO_4$, and 1.8 ascorbate. After at least 1 h recovery, slices were treated with 100 μM glutamate for 5 min and either collected immediately or replaced with fresh ACSF for 2 h before collection. All solutions were saturated with 95% O_2/5% CO_2.

Primary hippocampal culture preparation

To prepare primary hippocampal neurons, hippocampi were dissected from mixed sex rat pups (P0), dissociated in papain for 1 h, and plated at 100,000 cells/mL on glass coverslips for imaging and 500,000 cells/mL on culture dishes for biochemistry. At DIV 12-14, neurons were transfected with 1 μg total cDNA per well using Lipofectamine 2000 (Invitrogen), then imaged or treated and fixed 2-3 days later. For biochemical experiments, DIV16 neurons were treated and harvested via subcellular fractionation.

Chemical LTD and LTP stimulation

Chemical LTD (cLTD) was induced with 30 μM NMDA, 10 μM glycine, and 10 μM CNQX for 3 min. Chemical LTP (cLTP) was induced with 100 μM glutamate and 10 μM glycine for 45 sec. For imaging experiments, both treatments were followed by washout in aCSF. For biochemical experiments, treated cells were lysed immediately after stimulation.

GluA1 antibody labelling

An antibody directed against the extracellular N-terminal domain of GluA1 (Hiester et al., 2017; Kennedy et al., 2010) was affinity purified and conjugated to Alexa Fluor 647 dye using the Molecular Probes Alexa Fluor 647 Antibody Labeling Kit (Invitrogen, cat. no. A20186). Briefly, 100 μL of a 1.2 mg/mL anti-GluA1 antibody solution (containing 0.1 M sodium bicarbonate) was incubated with Alexa 647 Fluor reactive dye for 30 min at room temperature with gentle rocking. Alexa 647-conjugated anti-GluA1 antibody was separated from unbound dye by gel-filtration chromatography. The protein concentration after labeling was 0.6 mg/mL (in PBS, pH 7.2, 2 mM sodium azide) with 2.1 moles of dye per mole of protein. Labeled antibody was aliquoted and stored at -20°C.

Live imaging of GluA1 surface expression in primary hippocampal cultures

At DIV18, cultures were treated with unlabeled GluA1 antibody (1:300) to block existing surface receptors for 1 h. Then, neurons were exposed to either aCSF (vehicle control) or cLTP for 45 sec, and then washed with 5 volumes of aCSF over 1 min. Neurons were then treated with Alexa 647-conjugated GluA1 antibody (1:300) to label newly inserted surface receptors. After 20 min, neurons were again washed with 5 volumes of aCSF to remove unbound GluA1-647 antibody. Neurons were then imaged using a Axio Observer microscope (Carl Zeiss) fitted with a 63x Plan-Apo/1.4 numerical aperture (NA) objective, using 638 nm laser excitation and a CSU-XI spinning disk confocal scan head (Yokogawa) coupled to an Evolve 512 EM-CCD camera (Photometrics) and controlled using Slidebook 6.0 soft-ware (Intelligent Imaging Innovations [3i]; see also Woolfrey et al., 2018). Images of stained cells were captured with a 63x objective.

Image analysis

Regions of dendrites were masked using an experimentally determined threshold that captured the majority of GluA1 puncta while limiting the capture of noise. ROIs of individual GluA1 objects were then assessed for mean fluorescence intensity.

QUANTIFICATION AND STATISTICAL ANALYSIS

All data are shown as mean ± SEM. Statistical significance is indicated in the figure legends. Statistics were performed using Prism (GraphPad) software. Imaging experiments were obtained and analyzed using SlideBook 6.0 software. Western blots were analyzed using ImageJ (NIH). All data were tested for their ability to meet parametric conditions, as evaluated by a Shapiro-Wilk test for normal distribution and a Brown-Forsythe test (3 or more groups) or an F-test (2 groups) to determine equal variance. All comparisons between two groups met parametric criteria, and independent samples were analyzed using unpaired, two-tailed Student's t-tests. Comparisons between three or more groups meeting parametric criteria were done by one-way ANOVA with Tukey's post hoc test. Comparisons between three or more groups with two independent variables were assessed by two-way ANOVA with Bonferroni's post hoc test to determine whether there is an interaction and/or main effect between the variables.